Adaptive Isostable Reduction of Nonlinear PDEs With Time Varying Parameters

Dan Wilson and Seddik M. Djouadi

***Abstract*—Isostable reduction is a powerful technique for characterizing the transient behavior of a weakly forced, nonlinear dynamical systems in relation to a stable attractor. Practically, this reduction strategy requires small magnitude inputs so that the state remains close to the underlying attractor; when inputs become too large the reduction becomes unusable. Here, we develop an adaptive isostable coordinate framework that is valid for a continuous family of system parameters. Relations are derived that capture changes to the isostable coordinates in response to parameter changes. This information is subsequently used to define a reduction strategy valid for large magnitude but slowly varying inputs. The proposed reduction framework is compared to well-established linear and nonlinear proper orthogonal decomposition (POD) reduction techniques for simulations of the 1-dimensional nonlinear Burgers' equation with time-varying Dirichlet boundary conditions. In numerical simulations the proposed reduction strategy only requires a single mode to accurately capture system behavior. By contrast, the linear POD reduction performs poorly while the nonlinear POD strategy requires several modes to achieve comparable performance.**

***Index Terms*—Model/controller reduction, fluid flow systems.**

I. Introduction

TIME-VARYING partial differential equations (PDEs) govern a wide variety of physical phenomenon with applications including fluid flows [1], chemical processes [2], and biological systems [3]. In general, these systems are high-dimensional making them difficult to work with directly. As such, model reduction is often a necessary first step in the implementation and analysis of control algorithms.

The development of model reduction techniques for PDEs has been an active research area in recent years. Many reduction strategies are currently available such as proper orthogonal decomposition (POD) [4], balanced POD [5], empirical balanced truncation [6], dynamic mode decomposition (DMD) [7], Koopman decomposition [8], and global linear stability reduction [9]. While these reduction techniques work well in many applications, they can be difficult to apply to PDEs with dominant nonlinear terms. This becomes particularly apparent in fluid flow applications at high Reynolds numbers, where the nonlinear terms begin to dominate the behavior of the Navier-Stokes equations. In some nonlinear fluid flow applications, this difficulty can be overcome by explicitly considering the parametric dependence on the resulting reduced order models to enlarge the set of solutions that can accurately be considered [10], [11].

In this letter, we derive and investigate a new reduced modeling framework based on isostable coordinates. Isostable coordinates can be formally defined as level sets of Koopman eigenfunctions [12] and give a sense of the infinite time decay of an initial condition in the fully nonlinear basin of attraction of a stable attractor. This reduction framework has been applied to analyze and control dynamical systems near limit cycle [13], [14] and fixed point attractors [12], [15], [16]. Prior work has focused on using a single attractor to define isostable coordinates–by contrast this letter considers an extended isostable coordinate space that is valid for a family of stable attractors that emerge as nominal system parameters are changed. By considering this extended family of attractors, larger magnitude inputs can be considered making the proposed technique particularly attractive for systems with dominant nonlinear terms. This reduction framework is related to the strategy studied in [17], [18], whereby an extended phase space can be used to study the infinite time behavior of limit cycle oscillators in response to slowly varying inputs in ordinary differential equation models. By contrast, this letter is focused on understanding the transient behavior of PDEs near an underlying fixed point attractor. The existence of a set of fixed point attractors is essential for the proposed methodology–in situations where a stationary solution is not present techniques such as spectral POD or DMD may be more useful.

The organization of this letter is as follows: Section II provides necessary background on the notion of isostable coordinates as applied to PDEs. Section III details the proposed adaptive isostable reduction methodology. Section IV compares results using the proposed reduction strategy to a well-established POD reduction framework, and Section V gives concluding remarks.

Manuscript received March 2, 2020; revised May 9, 2020; accepted May 28, 2020. Date of publication June 10, 2020; date of current version June 24, 2020. This work was supported by the National Science Foundation under Award CMMI-1933583. Recommended by Senior Editor M. Guay. *(Corresponding author: Dan Wilson.)*

The authors are with the Department of Electrical Engineering and Computer Science, University of Tennessee, Knoxville, TN 37996 USA (e-mail: dwilso81@utk.edu; mdjouadi@utk.edu).

Digital Object Identifier 10.1109/LCSYS.2020.3001439

NOTATION

Let $\mathbb{R}$ and $\mathbb{C}$ be the sets of real and complex numbers, respectively. Let $\mathbb{R}^n$ denote the space of $n \times 1$ vectors with real entries. Ω denotes the domain of the PDEs considered, and $\partial\Omega$ represents its boundary. r denotes the spatial location, and t represents time. L^2 denotes the space of Lebesgue measurable and square integral functions defined on Ω or time depending on the context, with inner product $\langle \cdot, \cdot \rangle$. If A denotes a linear operator its adjoint is denoted by $A^\dagger$. $\nabla(\cdot)$ denotes the gradient of its argument.

II. BACKGROUND ON ISOSTABLE COORDINATES

Isostable coordinate frameworks have been used to characterize the decay of transient solutions to a stationary solution in nonlinear dynamical systems [12], [13], [14]. These isostable coordinates are formally related to level sets of Koopman eigenfunctions [12], [19], which can be used to analyze the infinite time behavior of a fixed point or limit cycle attractor in terms of an infinite set of exponentially decaying functions. An isostable reduction retains a subset of the slowly decaying Koopman eigenfunctions and truncates the rest. Here we provide a brief background on the use of isostable coordinates as applied to the reduction of PDEs.

To begin, consider a general PDE on the bounded domain Ω. Let $X(r,t) \in \mathbb{R}^\beta$ denote the state of the system at location r. We will consider separable Dirichlet boundary conditions of the form $X(r,t) = \sum_{j=1}^{N}(p_j(t)\eta_j(r))$ on $\partial\Omega$, i.e., the boundary conditions can be written as a linear combination of N linearly independent functions $\eta_j(r)$. Such a decomposition that arbitrarily closely approximates the terms of functions of separable variables t and r is always possible for finite energy solutions or control inputs by Hilbert-Schmidt theory [20]. Note that Neumann or mixed boundary conditions could also be used with straightforward modifications to the derivation to follow. This setup could, for instance, be used in aerodynamic flow control, e.g., to control flow separation with a finite number of actuators [21]. Defining $p = \begin{bmatrix} p_1 & \dots & p_N \end{bmatrix}^T \in \mathbb{R}^N$, let the dynamics of the PDE follow

$$\frac{\partial}{\partial t}X(r,t) = F(X(r,t), p(t)), \tag{1}$$

where F gives the dynamics as a function of the state and the (potentially) time-varying boundary conditions. For the purposes of this letter, Equation (1) is subject to the following assumptions: *Assumption A)* Equation (1) is well-posed; *Assumption B)* For any allowable boundary conditions Equation (1) has a stable stationary solution $X_{ss}(r,p)$ for which $F(X_{ss}(r,p),p) = 0$; *Assumption C)* The state $X(r,t)$ remains in the basin of attraction of $X_{ss}(r,p)$ for all time; *Assumption D)* For all allowable boundary conditions, the operator $J(r,p) \equiv \nabla F(X_{ss}(r,p),p)$ (i.e., the local linearization) exists as well as $J^\dagger(r,p)$ where † denotes the adjoint associated with $\langle \cdot, \cdot \rangle$, the L^2 inner product; *Assumption E) J* has a discrete spectrum (this is guaranteed if J is a compact operator) so that near $X_{ss}(r,p)$ a linearized solution to (1) can be written with a basis of eigenfunctions $v_j(r,p)$ and corresponding eigenvalues $\lambda_j(p)$ as

$$\xi(t, X(r), p) - X_{ss}(r,p) = \sum_{j=1}^{\infty} s_j(X(r))v_j(r,p)e^{\lambda_j(p)t}. \tag{2}$$

Above, $\xi(t, X(r), p)$ represents the flow of (1) at time t for a fixed p with initial state $X(r)$, and $s_j(X(r))$ gives the coordinate of the eigenfunction basis for the initial state; *Assumption F)* Each p_i takes values on a continuous and bounded domain; *Assumption G)* Each $\lambda_j(p)$ is a continuously varying function of p. By convention, we will sort these so that $0 > \max_p(\mathrm{Re}(\lambda_j(p))) \geq \max_p(\mathrm{Re}(\lambda_{j+1}(p)))$ where the maximum is taken over all allowable values of p. With this choice of ordering, $\lambda_1(p)$ is the eigenvalue corresponding to the eigenfunction with the slowest possible rate of decay. As done in [15], [16], [22], the spectrum of the linearized operator J can be used to define a basis of isostable coordinates. For a given value of p, for each $|\lambda_j(p)|$ that is small enough compared to $|\lambda_1(p)|$ (see [23]), one can define an associated isostable coordinate ψ_j that maps the state space to $\mathbb{C}$ (i.e., $X \mapsto \psi_j(X,p)$) according to the infinite time convergence to the stationary solution

$$\psi_j(X,p) = \lim_{t\to\infty} e^{-\lambda_j t}\int_\Omega Q_j^T(r,p)(\xi(t,X(r),p) - X_{ss}(r,p))dr, \tag{3}$$

where $Q_j(r,p)$ projects the solution onto $v_j(r,p)$ so that

$$\int_\Omega Q_j^T(r,p)v_k(r,p)dr = \begin{cases} 1, & \text{if } k = j, \\ 0, & \text{otherwise,} \end{cases} \tag{4}$$

where ^{T} denotes the vector transpose. The isostable coordinate definition given in (3) characterizes the limiting behavior as the solution approaches the stationary solution. More rapidly decaying isostable coordinates can be defined implicitly as level sets of Koopman eigenfunctions [19]. As illustrated in [15], [16], taking the time derivative of a given isostable coordinate for a solution that evolves under the flow of (1) (noting that ψ_j is a function of the time-varying state) each isostable coordinate decays exponentially according to $\frac{d\psi_j}{dt} = \lambda_j(p)\psi_j$ when p is held constant. Additionally, neglecting the nonlinear terms of the PDE (1) near the stationary solution, substituting (2) into (3) yields $\psi_j(X,p) = s_j(X(r))$ so that taking $t = 0$ in (2) one finds

$$\Delta X(r,p) \equiv X(r) - X_{ss}(r,p) = \sum_{j=1}^{\infty}\psi_j(X,p)v_j(r,p). \tag{5}$$

Note that in contrast with previous work on isostable coordinates, in the following sections we will consider how the isostable coordinates themselves depend on the parameter set p. This explicit dependence on the parameters will be exploited to define an adaptive isostable reduced coordinate framework.

III. An Adaptive Reduction Framework Based on Isostable Coordinates

A. Isostable Dynamics in Response to Parameter Changes

We provide the following derivation subject to the following assumption: *Assumption H)* For all allowable p both $X_{ss}(r,p)$ and each $\psi_j(X,p)$ are continuously differentiable with respect to r and p. Here, we consider the evolution of isostable coordinates along solutions of (1) with potentially nonstatic values of p. Changing to isostable coordinates using the chain rule for the functional derivatives, we have

$$\frac{d\psi_j}{dt} = \langle \nabla\psi_j, \partial X/\partial t\rangle + \sum_{i=1}^{N} \frac{\partial \psi_j}{\partial p_i}\frac{dp_i}{dt}, \tag{6}$$

where $\nabla\psi_j$ denotes the gradient of ψ_j evaluated at $X(r,t)$ when using the parameter set p. In order to simplify (6) further, recall that when p is held constant, $\frac{d\psi_j}{dt} = \lambda_j(p)\psi_j$ for all j. Using this fact, (6) implies

$$\langle \nabla\psi_j, \partial X/\partial t\rangle = \lambda_j(p)\psi_j. \tag{7}$$

For the remaining terms of (6), recalling the definition of ΔX from (5) we can write

$$\begin{aligned}\frac{\partial \psi_j}{\partial p_i} &= \left\langle \left[\frac{\partial \psi_j}{\partial \Delta X_1} \quad \cdots \quad \frac{\partial \psi_j}{\partial \Delta X_\beta}\right]^T, \partial \Delta X/\partial p_i \right\rangle \\ &= \langle \nabla\psi_j, \partial \Delta X/\partial p_i\rangle. \end{aligned}\tag{8}$$

In the above equation, $\partial\Delta X/\partial p_i$ characterizes the change in ΔX resulting from a change in the parameter p_i, and the second line is obtained by noting that for a fixed p_i, changes in X are identical to changes in ΔX. Additionally, changing p_i does not change the state $X(r,t)$ itself, but rather shifts $X_{ss}(r,p)$, i.e., the steady state reference. Therefore, from the definition (5) we can write

$$\frac{\partial \Delta X}{\partial p_i} = \lim_{dp_i\to 0} \frac{X_{ss}(r,p)|_{p_i} - X_{ss}(r,p)|_{p_i+dp_i}}{dp_i}, \tag{9}$$

with the other p_k taken at their nominal values for $k \neq i$. Substituting Equations (7)–(9) into (6), we can write

$$\frac{d\psi_j}{dt} = \lambda_j(p)\psi_j + \sum_{i=1}^{N}\left[\langle \nabla\psi_j, \partial\Delta X/\partial p_i\rangle \frac{dp_i}{dt}\right]. \tag{10}$$

In order to arrive at a reduction, we note that any isostable coordinates associated with large magnitude λ_j will decay rapidly to zero when excited by input; the most rapidly decaying isostable coordinates will be truncated by taking $\psi_j = 0$ for $j > \sigma$. This general truncation strategy has been used in previous work on PDEs [15], [16], [22] as well as when using isostable coordinates for describing systems of ordinary differential equations (ODEs) [14], [24], [25].

A final assumption will be made to relate the gradient of the isostable coordinates to the underlying equations: *Assumption I)* Each dp_i/dt is small for all i so that the non-truncated isostable coordinates (with dynamics that evolve according to (10)) remain small. With this assumption ΔX is small so that the gradient of each isostable coordinate $\nabla\psi_j$ can be well-approximated by its evaluation at the stationary solution $X_{ss}(r,p)$. The truncated isostable dynamics and corresponding output can then be written in the following form

$$\begin{aligned}\frac{d\Psi}{dt} &= \Lambda(p)\Psi + B(p)\dot{p},\\ X(r,t) &= X_{ss}(r,p) + \sum_{j=1}^{\sigma} \nu_j(r,p)\psi_j(t),\end{aligned}\tag{11}$$

where $\Psi \equiv \begin{bmatrix}\psi_1 & \dots & \psi_\sigma\end{bmatrix}^T$, $\Lambda(p)$ is a diagonal matrix comprised of the eigenvalues $\lambda_j(p)$, and $B(p) \in \mathbb{R}^{\sigma\times N}$ with j^{th} row and i^{th} column equal to $\langle \nabla\psi_j, \partial\Delta X/\partial p_i\rangle$ where $\nabla\psi_j$ is evaluated at $X_{ss}(r,p)$ and $\partial\Delta X/\partial p_i$ is evaluated according to (9). Here, the output equation in (11) is simply a truncated version of (5).

B. Computation of the Gradient of the Isostable Coordinates

The term $\nabla\psi_j$ is necessary to compute the reduced dynamical equations as part of (11). An equation for computing this gradient can be derived using a strategy similar to the one presented in [16] (which is itself based on a related strategy for PDEs with stable limit cycle solutions [26]). The following derivation takes a constant value for p. Consider some initial condition $X(r,t) = X_{ss}(r,p) + \Delta X(r,t,p)$, with $\Delta X(r,t,p)$ small. The dynamics can be written to leading order as

$$\frac{\partial \Delta X}{\partial t} = J(r,p)\Delta X(r,t,p) + O(||\Delta X(r,t,p)||^2). \tag{12}$$

Above, recall that $J(r,p)$ represents a local linearization with respect to $X_{ss}(r,p)$. Also, to leading order the isostable coordinate can be described as

$$\psi_j = \langle \nabla\psi_j, \Delta X(r,t,p)\rangle + O(||\Delta X(r,t,p)||^2), \tag{13}$$

with $\nabla\psi_j$ being a function of both r and p with the gradient evaluated at $X_{ss}(r,p)$. Noting that $X_{ss}(r,p)$ does not depend on time, taking the time derivative of (13) yields to leading order

$$\frac{d\psi_j}{dt} = \left\langle \nabla\psi_j, \frac{\partial \Delta X(r,t,p)}{\partial t}\right\rangle, \tag{14}$$

which can be simplified to

$$\begin{aligned}\lambda_j(p)\psi_j &= \langle \nabla\psi_j, J(r,p)\Delta X(r,t,p)\rangle \\ &= \langle J(r,p)^\dagger \nabla\psi_j, \Delta X(r,t,p)\rangle.\end{aligned}\tag{15}$$

To arrive at the second line in the above equation, recall above that † denotes the adjoint. Substituting (13) into the left hand side of (15) and simplifying yields

$$0 = \langle (J^\dagger(r,p) - \lambda_j(p)\mathrm{Id})\nabla\psi_j, \Delta X(r,t,p)\rangle, \tag{16}$$

where Id is an appropriately sized identity matrix. Since $\Delta X(r,t,p)$ is arbitrary, the following relation must hold:

$$0 = (J^\dagger(r,p) - \lambda_j(p)\mathrm{Id})\nabla\psi_j. \tag{17}$$

In other words, $\nabla\psi_j$ is an eigenfunction of $J^\dagger(r,p)$ associated with $\lambda_j(p)$. Recalling the relationship between each ν_j, its associated ψ_j and ΔX, along with (13), one can show that

$$\langle \nabla\psi_j, \nu_j(r,p)\rangle = 1 \tag{18}$$

is an appropriate normalization. For simple PDEs, it will sometimes be possible to write the adjoint explicitly in terms of $F(X(r,t),p(t))$ (see [26]). More commonly however, it will be necessary to first discretize (1) into a system of ODEs with appropriate boundary conditions [27]. Using this strategy, the system adjoint is simply the Hermitian transpose of the local Jacobian.

IV. Reduction of the 1-D Nonlinear Burgers' Equation

To illustrate the proposed reduction methodology, we consider the 1-D nonlinear Burgers' equation with a convective nonlinearity similar to that of the Navier-Stokes momentum equations:

$$\frac{\partial w}{\partial t} = \frac{1}{\mathrm{Re}}\frac{\partial^2 w}{\partial x^2} - w\frac{\partial w}{\partial x}, \tag{19}$$

where $x \in [0,1]$ is the domain, w is the state, and $\mathrm{Re} = 50$ is a viscosity term that is analogous to the Reynolds number from the Navier-Stokes equation. Koopman analysis has recently been applied to the Burgers' equation [28], [29] and has also been used in the solutions of related optimal control problems [30]. The present application extends on these ideas by explicitly considering the influence of changing boundary conditions on the level sets of the slowest decaying Koopman eigenfunctions (i.e., the isostable coordinates). As a final note, while Equation (19) itself is not particularly complicated (in fact, the Cole-Hopf transformation [31], [32] can be used to find an exact solution) it is often used as a test bed for development of reduced order modeling strategies.

To implement the model simulations, the domain is discretized into 202 elements using a central-space scheme. The resulting system of equation is simulated using the ode15s scheme in MATLAB. For this model, we let $p(t) = \begin{bmatrix} w_L(t) & w_R(t) \end{bmatrix}^T$ where $w_L(t)$ and $w_R(t)$ are time-varying boundary conditions at $x = 0$ and $x = 1$, respectively. Steady state solutions X_{ss}, decay rates of the eigenvalues, and corresponding eigenfunctions are computed numerically by taking constant values of $w_L \in [-0.2, 0.2]$ and $w_R \in [-0.2, 0.2]$. Likewise, gradients of the isostable coordinates are computed numerically by identifying the required eigenfunctions from (17) after discretizing the operator. Panel A of Figure 1 shows how the principle eigenvalues change for different values of w_L when w_R is set to zero. Panel B shows the corresponding steady state solutions. Panel C gives the corresponding values of $d\psi_1/dw_L$ and $d\psi_1/dw_L$ that comprise $B(p)$ from (11) calculated when $w_R = 0$. Panel D shows how the state changes as a function of the principle isostable coordinate, ψ_1, for a given set of boundary conditions when all other isostable coordinate are taken to be zero.

A. Comparison to Proper Orthogonal Reduction Strategies

A POD strategy will be compared to the adaptive isostable reduction strategy (11). The POD framework attempts to extract a small set of reduced order modes from a representative set of solution snapshots [1], [4]. Provided the

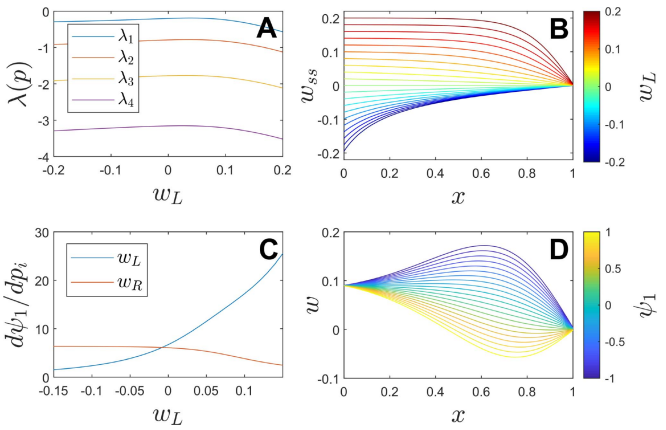

Fig. 1. Illustration of terms of the adaptive isostable reduced equations (11) for the 1-D Burgers' equation. Panels A, B, and C illustrate the principle eigenvalues, steady state solutions, and terms of $B(p)$ taking $w_R = 0$ and varying w_L. Taking $w_L = 0.09$ and $w_R = 0$, panel D shows $X_{ss} + \psi_1 v_1$ giving a sense of how the state depends on the principle isostable coordinate.

underlying PDE model is known, the POD modes can be used to generate a dynamical model. Briefly, to generate data snapshots for the POD based model, Equation (19) is simulated for 18000 time units with left boundary condition $w_L(t) = 0.15\sin(2\pi t/(300 + 0.05t))$ for $t < 6000$, $w_L(t) = 0$ for $6000 \le t < 12000$ and $w_L(t) = 0.15\sin(2\pi t/(300 + 0.05(t - 12000)))$ for $12000 \le t < 18000$. Likewise, the right boundary condition is taken to be $w_R(t) = 0.15\sin(2\pi t/(300+0.1t))$ for $t < 6000$, $w_R(t) = 0.15\sin(2\pi t/(300+0.1(t-6000)))$ for $6000 \le t < 12000$ and $w_R(t) = 0$ for $12000 \le t < 18000$. These oscillating boundary conditions are chosen to provide a representative sample of data from which to construct the POD basis. Snapshots $x_i \in \mathbb{R}^{202}$ are taken every 0.01 time units and stacked side-by-side into the matrix $X = \begin{bmatrix} x_1 & x_2 & \dots \end{bmatrix}$. A POD basis is extracted by finding the eigenvalues and eigenvectors of the covariance matrix XX^T. The eigenvectors of XX^T are the POD modes, ϕ_i, and those with the largest corresponding eigenvalues λ_i^{POD} (not to be confused with the eigenvalues characterizing the decay of isostable coordinates) capture more of the temporal fluctuations in the data set. A reduced POD model can be obtained by choosing the order ζ such that

$$\chi \equiv \sum_{j=1}^{\zeta} \lambda_j^{\mathrm{POD}} \Big/ \sum_{j=1}^{202} \lambda_j^{\mathrm{POD}} \approx 1. \tag{20}$$

Left panels of Figure 2 show the first four resulting POD modes. When taking $\zeta = 4$, χ is computed to be 0.99975 (i.e., the basis contains 99.975 percent of the total energy) indicating that these four modes provide an adequate representation of the snapshot data. Indeed, as illustrated in the right panels of Figure 2, simulating the full model (19) according to $w_L(t) = 0.15\sin(2\pi t/350)$ and $w_R(t) = 0.075\sin(2\pi t/200)$, the POD basis accurately captures the spatial structure of the resulting data when using 4 modes. Note that the right panels of Figure 2 show a projection of $w(x,t)$ onto the POD basis, i.e., using $\Phi(\Phi^T w(x,t))$ where $\Phi = \begin{bmatrix} \phi_1 & \phi_2 & \phi_3 & \phi_4 \end{bmatrix}$. This projection is not computed according to any reduced model dynamics.

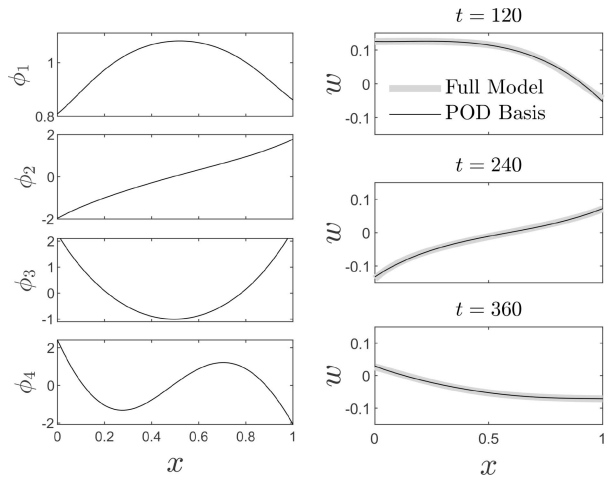

Fig. 2. The left panels show the principle modes of the POD basis obtained using the strategy described in the text. The right panels show a projection of the solution $w(x, t)$ onto a 4 mode POD basis.

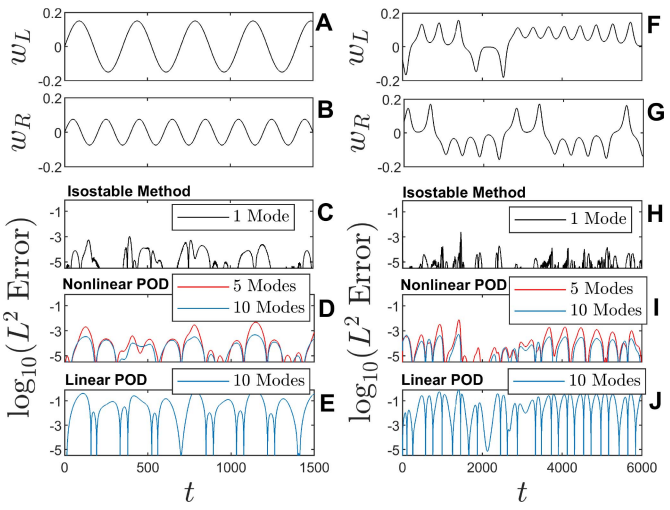

Fig. 3. Panels A and B show the sinusoidally time-varying Dirichlet boundary conditions. The resulting full model output is compared to the reduced model outputs in panels C-E. Panels F and G show time-varying boundary conditions that are determined from independently generated outputs of the Lorenz equations. Panels H-J compare the resulting reduced and full model outputs. In each simulation, the adaptive isostable reduced model only requires a single mode and achieves better performance than the other reduced models considered.

A dynamical model can be derived using a strategy detailed in [33], [34] by letting $w(t, x) \approx \sum_{j=1}^{\zeta} \alpha_j(t)\phi_j(x)$ where α_j denotes the coefficient of the j^{th} POD mode. Taking the inner product of each ϕ_i with both sides of the PDE (19), integrating over the domain, and exploiting the orthogonality of the POD modes, the dynamics of the α_j coefficients evolve according to

$$\begin{aligned} \dot{\alpha} &= A\alpha + Bp + \mu(\alpha), \\ w(x, t) &= \sum_{j=1}^{\zeta} \phi_j(x)\alpha_j(t), \end{aligned} \tag{21}$$

where $\alpha = \begin{bmatrix}\alpha_1 & \dots & \alpha_\zeta\end{bmatrix}^T$, $A \in \mathbb{R}^{\zeta\times\zeta}$, and $B \in \mathbb{R}^{\zeta\times 2}$ characterize the linear terms of the reduction, $\mu(\alpha)$ contains terms that are quadratic in the POD coefficients, and p was defined earlier. The terms of A, B, and μ are explained in [34] along with full details of the derivation of (21). The results from the adaptive isostable reduction (11) will be compared to both the fully nonlinear POD model (21) and the linearization of (21) about its stationary solution.

B. Comparison Between Reduced Adaptive Isostable and POD Model Dynamics

The adaptive isostable (11), nonlinear POD reduction (21), and the linearized POD reduction are compared in terms of their abilities to replicate the full system behavior of the 1-D Burgers' equation (19). Trials using two separate sets of inputs are used. The first inputs are $w_L(t) = 0.15\sin(2\pi t/350)$ and $w_R(t) = 0.075\sin(2\pi t/200)$ with results shown in panels A-E of Figure 3. Panels C-E show the L^2 error defined as $E(t) = \int_\Omega (w_{\text{red}}(x, t) - w_{\text{full}}(x, t))^2 dx$ where $w_{\text{full}}(x, t)$ is the full solution simulated according to (19) and $w_{\text{red}}(x, t)$ is the reduced model output. For the second set of simulations, the inputs are $w_L(t) = 0.01I_1(t)$ and $w_R(t) = 0.01I_2(t)$, where $I_1(t)$ and $I_2(t)$ are independently generated outputs of the variable x from simulations of the chaotic Lorenz equation [35], $\dot{x} = 10(y - x)/600$, $\dot{y} = (x(28 - z) - y)/600$, and $\dot{z} = (xy - 8z/3)/600$. The temporal scaling in the Lorenz equations is included so that the inputs vary sufficiently slowly. The inputs for the second set of trials are shown in Panels F and G of Figure 3. Panels C-E show the L^2 error of the reduced models. In each simulation, the single mode adaptive isostable reduced strategy significantly outperforms the linear POD reduction framework. Additionally, the adaptive isostable reduced method requires several modes to achieve comparable results to capture the behavior in response to the sinusoidal stimulation–for input based on the Lorenz model output, the single mode adaptive isostable reduced model still performs better than the nonlinear POD strategy that uses 10 modes.

It is important to emphasize here that while the POD reduction strategy provides an optimal orthogonal basis (in an energy sense) for representing the output from the underlying model (19), the POD framework does not perfectly match the dynamics. When using ten modes, the amount of energy captured according to (20) is $\chi = 0.99999998$, in other words, the 10 mode POD basis captures virtually all of the energy. Nevertheless, the resulting linearized version of (21) performs poorly while the nonlinear version does not perform as well as the single mode adaptive isostable reduced model.

V. Conclusion

In this letter, we proposed an adaptive isostable reduction strategy that is valid for slowly varying model inputs. This framework is an extension of the isostable coordinate framework [12], [13], [16] which characterizes the infinite-time decay of solutions towards an attractor. The adaptive isostable strategy illustrated here considers the isostable reduced coordinates for a continuous family of system parameters; by understanding how parameter changes influence these isostable coordinates, a reduced order model can be obtained that is more accurate than the nonlinear POD strategy used for comparison purposes. While the specific model (19) is relatively

simple, this methodology could be applied straightforwardly to more complicated systems provided the necessary terms of the reduction (11) can be computed.

In contrast to other recently developed isostable reduction strategies, [15], [16], [22], the proposed reduction framework is valid for arbitrarily large inputs. This can be particularly useful for systems with dominant nonlinear terms where large inputs drive the state far from the underlying attractor. The proposed isostable reduction strategy is related to the framework given in [17] which studied an extended phase space in ODE models of limit cycle oscillators to characterize the timing of oscillations subject to large magnitude but slowly-varying inputs. In contrast to [17], this letter is focused on understanding the temporal decay of solutions to a steady state solution in order to characterize the state dynamics.

There are many opportunities for extension of the proposed method. It may be possible to leverage strategies from [25] to compute the necessary terms of (11) to higher order accuracy in the isostable coordinates thereby giving a better picture of the behavior as the magnitude of the time derivative of the input becomes larger. Additionally, while continuously changing boundary conditions are considered here, many practical applications have boundary conditions that vary discretely and it would be worthwhile to consider how to extend the proposed method for use in these situations. A drawback of the proposed adaptive reduction presented here is that it requires knowledge of the full system equations in order to compute the adjoint of the local linearization from (12). Even if the full equations are known, it may be computationally difficult to compute the adjoint for more complicated problems. By contrast, POD and DMD can still be implemented without knowledge of the full model equations using snapshot data. It would be useful to develop strategies to infer the necessary terms of the adaptive isostable reduced equations from similar snapshot data. These issues will be the subject of future investigation.

REFERENCES

[1] K. Taira *et al.*, "Modal analysis of fluid flows: An overview," *AIAA J.*, vol. 55, pp. 4013–4041, Dec. 2017.

[2] C. W. Gardiner, *Handbook of Stochastic Methods: For Physics, Chemistry and the Natural Sciences*. Berlin, Germany: Springer, 2004.

[3] E. Brown, J. Moehlis, and P. Holmes, "On the phase reduction and response dynamics of neural oscillator populations," *Neural Comput.*, vol. 16, no. 4, pp. 673–715, 2004.

[4] P. Holmes, J. L. Lumley, G. Berkooz, and C. W. Rowley, *Turbulence, Coherent Structures, Dynamical Systems and Symmetry*. New York, NY, USA: Cambridge Univ. Press, 1996.

[5] C. Rowley, "Model reduction for fluids, using balanced proper orthogonal decomposition," *Int. J. Bifurcation Chaos Appl. Sci. Eng.*, vol. 15, no. 3, pp. 997–1013, 2005.

[6] S. Djouadi, C. Camphouse, and J. Myatt, "Reduced order models for boundary feedback flow control," in *Proc. Amer. Control Conf.*, Seattle, WA, USA, 2008, pp. 4005–4010.

[7] P. J. Schmid, "Dynamic mode decomposition of numerical and experimental data," *J. Fluid Mech.*, vol. 656, pp. 5–28, Aug. 2010.

[8] M. Budišić, R. Mohr, and I. Mezić, "Applied Koopmanism," *Chaos Interdiscipl. J. Nonlinear Sci.*, vol. 22, no. 4, 2012, Art. no. 047510.

[9] V. Theofilis, "Advances in global linear instability analysis of nonparallel and three-dimensional flows," *Progr. Aerosp. Sci.*, vol. 39, no. 4, pp. 249–315, 2003.

[10] A. Hay, J. T. Borggaard, and D. Pelletier, "Local improvements to reduced-order models using sensitivity analysis of the proper orthogonal decomposition," *J. Fluid Mech.*, vol. 629, pp. 41–72, Jun. 2009.

[11] M. Bergmann, C.-H. Bruneau, and A. Iollo, "Enablers for robust POD models," *J. Comput. Phys.*, vol. 228, no. 2, pp. 516–538, 2009.

[12] A. Mauroy, I. Mezić, and J. Moehlis, "Isostables, isochrons, and Koopman spectrum for the action–angle representation of stable fixed point dynamics," *Physica D, Nonlinear Phenomena*, vol. 261, pp. 19–30, Oct. 2013.

[13] D. Wilson and B. Ermentrout, "Greater accuracy and broadened applicability of phase reduction using isostable coordinates," *J. Math. Bio.*, vol. 76, nos. 1–2, pp. 37–66, 2018.

[14] D. Wilson, "A data-driven phase and isostable reduced modeling framework for oscillatory dynamical systems," *Chaos Interdiscipl. J. Nonlinear Sci.*, vol. 30, no. 1, 2020, Art. no. 013121.

[15] D. Wilson and S. Djouadi, "Isostable reduction and boundary feedback control for nonlinear convective flows," in *Proc. 58th IEEE Conf. Decis. Control*, Nice, France, 2019, pp. 2138–2143.

[16] D. Wilson and J. Moehlis, "Isostable reduction with applications to time-dependent partial differential equations," *Phys. Rev. E, Stat. Phys. Plasmas Fluids Relat. Interdiscip. Top.*, vol. 94, no. 1, 2016, Art. no. 012211.

[17] W. Kurebayashi, S. Shirasaka, and H. Nakao, "Phase reduction method for strongly perturbed limit cycle oscillators," *Phys. Rev. Lett.*, vol. 111, no. 21, 2013, Art. no. 214101.

[18] Y. Park and B. Ermentrout, "Weakly coupled oscillators in a slowly varying world," *J. Comput. Neurosci.*, vol. 40, no. 3, pp. 269–281, 2016.

[19] I. Mezić, "Spectrum of the Koopman operator, spectral expansions in functional spaces, and state-space geometry," *J. Nonlinear Sci.*, pp. 1–55, Dec. 2019. [Online]. Available: https://doi.org/10.1007/s00332-019-09598-5

[20] S. Djouadi, "On the optimality of the proper orthogonal decomposition and balanced truncation," in *Proc. 47th IEEE Conf. Decis. Control*, Cancun, Mexico, 2008, pp. 4221–4226.

[21] S. Collis, R. Joslin, A. Seifert, and V. Theofilis, "Issues in active flow control: Theory, control, simulation, and experiment," *Progr. Aerosp. Sci.*, vol. 40, pp. 237–289, Jul. 2004.

[22] D. Wilson, S. Sahyoun, P. Kreth, and S. Djouadi, "Investigating the underlying dynamical structure of supersonic flows using effective model reduction," in *Proc. Amer. Control Conf.*, Jul. 2020.

[23] M. D. Kvalheim and S. Revzen, "Existence and uniqueness of global Koopman eigenfunctions for stable fixed points and periodic orbits," 2019. 2019. [Online]. Available: arXivpreprint 1911.11996.

[24] B. Monga and J. Moehlis, "Optimal phase control of biological oscillators using augmented phase reduction," *Biol. Cybern.*, vol. 113, nos. 1–2, pp. 161–178, 2019.

[25] D. Wilson, "Phase-amplitude reduction far beyond the weakly perturbed paradigm," *Phys. Rev. E, Stat. Phys. Plasmas Fluids Relat. Interdiscip. Top.*, vol. 101, no. 2, 2020, Art. no. 022220.

[26] H. Nakao, T. Yanagita, and Y. Kawamura, "Phase-reduction approach to synchronization of spatiotemporal rhythms in reaction-diffusion systems," *Phys. Rev. X*, vol. 4, no. 2, 2014, Art. no. 021032.

[27] J. Keener and J. Sneyd, *Mathematical Physiology*. New York, NY, USA: Springer, 1998.

[28] J. Page and R. R. Kerswell, "Koopman analysis of Burgers equation," *Phys. Rev. Fluids*, vol. 3, no. 7, 2018, Art. no. 071901.

[29] N. J. Kutz, J. L. Proctor, and S. L. Brunton, "Applied Koopman theory for partial differential equations and data-driven modeling of spatio-temporal systems," *Complexity*, vol. 2018, p. 16, Dec. 2018.

[30] S. Peitz and S. Klus, "Koopman operator-based model reduction for switched-system control of PDEs," *Automatica*, vol. 106, pp. 184–191, Aug. 2019.

[31] E. Hopf, "The partial differential equation $u_t + uu_x = \mu_{xx}$," *Commun. Pure Appl. Math.*, vol. 3, no. 3, pp. 201–230, 1950.

[32] J. D. Cole, "On a quasi-linear parabolic equation occurring in aerodynamics," *Quart. Appl. Math.*, vol. 9, no. 3, pp. 225–236, 1951.

[33] R. C. Camphouse and J. Myatt, "Reduced order modelling and boundary feedback control of nonlinear convection," in *Proc. AIAA Guid. Navig. Control Conf. Exhibit*, 2005, p. 5844.

[34] S. Sahyoun, S. Djouadi, and T. Lancewicki, "Nonlinear optimal control for reduced order quadratic nonlinear systems," in *Proc. 22nd Int. Symp. Math. Theory Netw. Syst.*, 2016, pp. 334–339.

[35] A. Pikovsky, M. Rosenblum, and J. Kurths, *Synchronization: A Universal Concept in Nonlinear Sciences*, vol. 12. Cambridge, U.K.: Cambridge Univ. Press, 2003.